Improving resolution-sensitivity trade off in sub-shot noise quantum imaging (EP)

I. Ruo-Berchera (iD), A. Meda (iD), E. Losero (iD), A. Avella (iD), N. Samantaray, and M. Genovese (iD)

COLLECTIONS

Paper published as part of the special topic on Quantum Sensing with Correlated Light Sources
Note: This paper is part of the APL Special Collection on Quantum Sensing with Correlated Light Sources.

(EP) This paper was selected as an Editor's Pick

View Online   Export Citation   CrossMark

Improving resolution-sensitivity trade off in sub-shot noise quantum imaging (EP)

I. Ruo-Berchera,[1,a)] (iD) A. Meda,[1] (iD) E. Losero,[1] (iD) A. Avella,[1] (iD) N. Samantaray,[2] and M. Genovese[1] (iD)

AFFILIATIONS

[1]INRIM, Istituto Nazionale di Ricerca Metrologica, Strada delle Cacce 91, Torino 10135, Italy
[2]Quantum Engineering Technology Labs, H. H. Wills Physics Laboratory and Department of Electrical and Electronic Engineering, University of Bristol, Bristol BS8 1FD, United Kingdom

Note: This paper is part of the APL Special Collection on Quantum Sensing with Correlated Light Sources.
a)Author to whom correspondence should be addressed: i.ruoberchera@inrim.it

ABSTRACT

One of the challenges of quantum technologies is realizing the quantum advantage, predicted for ideal systems, in real applications, which have to cope with decoherence and inefficiencies. In quantum metrology, sub-shot-noise quantum imaging (SSNQI) and sensing methods can provide genuine quantum enhancement in realistic situations. However, wide-field SSNQI schemes realized so far suffer a trade-off between the resolution and the sensitivity gain over a classical counterpart: small pixels or integrating area are necessary to achieve high imaging resolution, but larger pixels allow a better detection efficiency of quantum correlations, which means a larger quantum advantage. Here, we show how the SSNQI protocol can be optimized to significantly improve the resolution without giving up the quantum advantage in sensitivity. We show a linear resolution improvement (up to a factor 3) with respect to the simple protocol used in previous demonstrations.

Imaging delicate systems using a small number of incident photons with true and significant quantum enhanced sensitivity is extraordinarily important for applications, from biology and medicine to fundamental physics research. The first proof of principle of sub-shot-noise quantum imaging (SSNQI) of a 2D absorption/transmission mask was given in 2010,[1] and in 2017, some of us reported the realization of the first wide-field sub-shot noise microscope.[2] It is based on spatially multi-mode non-classical photon number correlations of twin-beam states, produced by spontaneous parametric downconversion (SPDC) and detected by a high quantum efficiency CCD camera.[3–7] The sample (2D mask) is probed by one beam with a certain level of quantum fluctuations, so that the detected image is affected by a noise pattern. However, a second reference beam, locally correlated in the photon number with the first one, generates at the detector an identical noise pattern. In this way, one can simply remove the noise by subtraction. The microscope of Ref. 2 produces real-time images of several thousand pixels and 5 μm of resolution even though the actual quantum enhancement in sensitivity compared to the best classical protocol is effective at larger spatial scales. In fact, in this technique, there is a clear trade-off between the resolution and the quantum enhancement, due to the fact that pixels

or integrating areas smaller than the characteristic size of the spatial modes do not intercept all the correlated photons between pairs of conjugated modes. With the aim of improving the performance of this technique, in Ref. 8, we studied in deep detail the problem of absorption estimation by photon counting toward the ultimate quantum limit, taking into account experimental inefficiencies. In particular, we analytically showed the advantage of the optimized estimator proposed in Ref. 9, especially in the case of limited detection efficiency. This estimator does not involve modification of the setup, but only a slightly different use of the data and a pre-calibration of the system.

Here, we use this estimation protocol to shift the resolution-sensitivity trade-off of the SSNQI, improving the resolution of a factor 3 in the best case. It turns out that in this way, it is in principle possible to obtain SSNQI at the Rayleigh resolution limit.

The lower bound to the uncertainty in a loss estimation for classical probes, i.e., mixture of coherent states, is[10]

$$U_{coh} \simeq [(1-\alpha)/\langle n_P \rangle]^{1/2}, \qquad (1)$$

where $\langle n_P \rangle$ is the mean number of photons of the probe and $0 \le \alpha \le 1$ is the loss induced by the sample. Only for high losses, the uncertainty can be arbitrarily small, while in the case of a faint loss, one retrieves the

expression $U_{snl} = \langle n_P \rangle^{-1/2}$, usually referred to as the "shot-noise-limit" (SNL).

In general, excluding adaptive strategies where the limit is still unknown,[10] the ultimate quantum limit (UQL) of sensitivity for a single mode probe is $U_{uql} \simeq \sqrt{\alpha}\, U_{coh}$,[11,12] which scales much more favorably than the classical bound for small losses. Several quantum states have been demonstrated to reach, in principle, this ultimate limit: single mode squeezed vacuum, with the detection strategy based on photon counting and Gaussian operations, for small losses and a small number of photons;[11] Fock states $|n\rangle$, with photon counting, unconditionally for any α but if $\langle n_P \rangle \geq 1$;[12] and two-mode squeezed vacuum (TMSV) state with photon counting,[13] unconditionally for any loss and all energy regimes.[14] TMSV is the photon number entangled state,

$$|TMSV\rangle_{R,P} = \sum_n c_n |n\rangle_R |n\rangle_P, \qquad (2)$$

where the subscripts "R" and "P" represent two correlated modes, and the probability amplitude is $c_n \propto \sqrt{\langle n_P \rangle^n / (\langle n_P \rangle + 1)^{n+1}}$, with $\langle n_P \rangle$ being the mean number of photons in each of the two modes.

On the experimental side, a seminal proposal on the absorption measurement with photon pairs produced by SPDC, i.e., using a faint TMSV state, was given already in 1986[15] and a sub-shot-noise measurement of modulated absorption using SPDC has been realized few years later.[16] More recently, quantum enhanced absorption measurements have been performed by post-selected heralded single photon Fock states[17] and also through an active feed-forward driven by an optical shutter.[18] In those cases, on/off single photon detectors have been used. However, the higher genuine quantum enhancement has been achieved in experiments exploiting the low noise intensity measurement (photon counting), taking advantage of the high quantum efficiency and small electronic noise of modern CCD cameras.[8,9] An enhancement of the order of 50% with respect to the classical bound has been achieved for the same number of detected photons and 32% if perfect detection efficiency is considered only for the classical scheme.[8] With these detectors, which also provide flexible spatial resolution and exploiting the spatially multimode emission of traveling wave SPDC, it has been possible to devise,[6] and realize[1,2,19] wide field SSNQI schemes where a 2D amplitude mask is recovered by parallel multi-parameter absorption/transmission estimation.

Reference 8 reports a systematic study of the performance achieved by several possible estimation strategies based on the detected number of photons jointly measured in the probe, named N'_P in the presence of the sample, N_P in the absence of it, and the reference N_R. In summary, three estimators have been considered there:

- *Ratio*, as used, for example, in Ref. 15,

$$S_\alpha = 1 - \gamma \frac{N'_P}{N_R}, \qquad (3)$$

- *Subtraction*, considered for SSNQI,[1,2,6]

$$S''_\alpha = \frac{N_R - \gamma N'_P}{\langle N_R \rangle}, \qquad (4)$$

- *Optimized subtraction*, considered in Refs. 16 and 9,

$$S'_\alpha = 1 - \frac{N'_P - k_{opt}(N_R - \langle N_R \rangle)}{\langle N_P \rangle}. \qquad (5)$$

The factor $\gamma = \langle N_R \rangle / \langle N_P \rangle$ is introduced to account for unbalancing between the mean energy detected in the reference arm and in the probe arm without the sample. It can be evaluated in a pre-calibration of the apparatus, which should last long enough to provide an accurate determination of γ. In the third estimator, the factor k_{opt} must be optimized as a function of the physical parameters of the system. In particular, it turns out that k_{opt} is a function of the detection efficiencies of the channels and the local excess noise. Clearly, each of the three estimation strategies is based on the idea that the common photon number fluctuations of the probe and reference beam can be suppressed or at least mitigated by a direct comparison. However, in terms of the uncertainty, they behave differently. For the general expressions, obtained propagating the uncertainty on the photon numbers N'_P, N_P, and N_R, the reader should refer to Ref. 8. For simplicity, here we consider the same detection efficiency η_d in the two arms, i.e., $\gamma = 1$. Moreover, we consider a large number $M \gg 1$ of spatiotemporal realizations of TMSV states in Eq. (2) (here collectively named the twin-beam state), detected by each pixel in the measurement time, where $\langle n_P \rangle = \langle N_P \rangle / (\eta_d \cdot M)$. In the following, we will consider the limit of $M \gg \langle N_P \rangle \gg 1$. On one side, this condition takes into account the typical experimental situation where the detectors have a limited bandwidth, and the source has a low brightness, $\langle n_P \rangle \ll 1$. On the other side, it allows us to consider the statistics of $\langle N_P \rangle$, in general, multi-thermal, approaching a Poissonian distribution, where each pixel can be considered statistically independent of others in the same arm. In this limit, the expressions of the uncertainty on α can be written as (see Ref. 8 for more details)

- Uncertainty of the *Ratio*

$$\Delta^2 S_\alpha \simeq \frac{U_{uql}^2}{\eta_d} + 2 \frac{(1-\alpha)^2}{\langle N_P \rangle} (1-\eta). \qquad (6)$$

- Uncertainty of the *Subtraction*

$$\Delta^2 S''_\alpha = \frac{U_{uql}^2}{\eta_d} + \frac{2(1-\alpha)(1-\eta) + \alpha^2}{\langle N_P \rangle}. \qquad (7)$$

- Uncertainty of the Optimized subtraction

$$\Delta^2 S'^{(TWB)}_{\alpha,\eta} = \frac{U_{uql}^2}{\eta_d} + \frac{(1-\alpha)^2}{\langle N_P \rangle} (1-\eta^2). \qquad (8)$$

In the above equations, the parameter η ($0 < \eta \leq 1$) is related to the noise reduction factor $NRF = \Delta^2(N_P - N_R)/\langle N_P + N_R \rangle$[20–22] by the relation $NRF = 1 - \eta$. The NRF represents the level of correlation of the joint detected photon number distributions and can be estimated experimentally. For $0 \leq NRF < 1$, the correlations are non-classical. Here, η can be interpreted as the efficiency in detecting correlated photons, i.e., the probability that for a photon detected in a certain pixel in the probe arm, its twin photon is detected in the correlated pixel in the reference arm. Thus, it can be written as the product of the channel detection efficiency and a collection efficiency term, $\eta = \eta_d \cdot \eta_c$. The collection efficiency η_c takes into account for the fact that in real systems, correlated modes cannot be always perfectly detected. In the ideal situation, assuming $\eta = 1$, both the *Ratio* in Eq. (3) and the *Optimized* estimator in Eq. (5) reach the UQL, while the *Subtraction* estimator in Eq. (4) approaches the UQL only asymptotically for a small value of the loss α. However, another significant

difference appears in the non-ideal detection case, because of the different dependence of Eqs. (6)–(8) from η. In particular, for the *Ratio* and the *Subtraction* estimators, the positive additive term exceeding the UQL is $\propto 2(1 - \eta)$, which is larger than the one for the *Optimized* case $\propto (1 - \eta^2)$, for any value of η. This means that the *Optimized* estimator works always better than the others and that this advantage is larger for low efficiency η. For example, rewriting Eqs. (6)–(8) in terms of the classical bound U_{coh} of Eq. (1), it is easy to see that the quantum advantage for the *Ratio* or the *Subtraction* estimators starts from $\eta \geq 0.5$. In contrast, the twin beam state together with the *Optimized subtraction* protocol performs always better than the classical bound. In the following, we will show how this feature of the *Optimized* estimator is particularly suited for the SSNQI improvement also in terms of resolution.

In wide-field imaging realizations with SPDC,[1,2] the spatial pattern in the far field of the emission, where the transmitting mask is placed, is a continuous distribution of independent spatial modes with a certain coherence area given by the Fourier transform of the pump beam profile. This plane is then projected at the pixel's matrix of the detector chip, where probe and reference beams are detected in two different regions. Figure 1 describes the details of our experimental setup.

The pixel size, or, more in general, the elementary integration area in one arm, should be large enough to collect a certain number of modes. It is straightforward that if a photon is detected in a certain
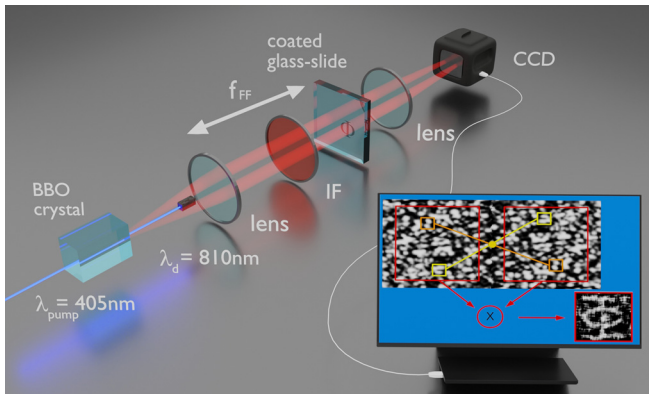

FIG. 1. A multi-mode twin-beam state is produced through the SPDC, pumping a non-linear crystal (Type-II-Beta-Barium-Borate, BBO) with a CW laser-beam (100 mW at $\lambda_{pump} = 405$ nm). The down-converted photons around the degeneracy wavelength, $\lambda_d = 810$ nm, are spectrally selected using an interferential filter [IF, (800 ± 20 nm)]. The resulting state can be approximated as a tensor product of independent TMSV states as $|\Psi\rangle = \otimes_{q,\lambda} |TMSV\rangle$, where q and λ are the transverse momentum and the wavelength of one of the two photons produced, while momentum and wavelength of the other photon are fixed by energy and momentum conservation. The far field is obtained at the focal plane of a lens with $f_{FF} = 1$ cm focal length, where the correlation in momentum is converted into correlation between symmetric positions. A coated glass-slide with a 2D absorbing mask, realized as a thin titanium deposition of absorption $\alpha \sim 1\%$, is placed in this plane. This is then imaged (magnification of 7.8) to the chip of a charge-coupled-device (CCD) camera with a nominal quantum efficiency of 95% at 810 nm and a pixel size of 13 μm. We perform a 3 × 3 pixel binning, to set the resolution to 5 μm at the object plane, which matches the measured cross correlation length. The acquisition time of a single frame is ~100 ms, the number of temporal modes per pixel per frame is ~10^{11}, and the number of photo-counts is $\langle N \rangle = 10^3$. The estimated detection efficiency is $\eta_d = 0.81$.

pixel in the probe arm, the corresponding pixel in the reference arm should be at least as large as the correlation area; otherwise, correlated photons would fall outside the pixel, representing an effective loss when pixel to pixel correlations are considered. Moreover, a photon detected close to the edge between a pixel and its neighbors has its twin photon detected with only 50% average probability in the symmetric pixel in the reference arm. Both these contributions to losses are taken into account by η_c, enclosed in η in Eqs. (6)–(8). In the conditions of our experiment, and assuming a perfect alignment, η_c is solely related to the ratio $X = d/2r$, with d being the pixel size and r the radius of the correlation area. The details of this model can be found in previous literature studies.[2,23,24]

In Fig. 2, we report the experimental *NRF* as a function of the spatial resolution, i.e., the minimum dimensions of a detail to be appreciated, which corresponds to the size of the integration area d. The *NRF* decreases with increasing d (or X), as long as the collection efficiency η_c increases and saturates the value $1 - \eta_d$ for $d > 50$ (where $\eta_c \approx 1$). In the same figure, the quantum enhancement in the sensitivity is also reported, as a function of the resolution. Of course, in general, a suitable trade-off between the resolution d and the sensitivity should be found. The dashed red curve represents the quantum advantage of the twin beam using the *Subtraction* estimator. It is evaluated as $U_{coh}/\sqrt{\Delta^2 S_\alpha''}$, replacing in Eqs. (1) and (7) the values of *NRF* $= 1 - \eta$ and α with their experimentally estimated values. The solid red line represents the corresponding quantum enhancement for the *Optimized* estimation, e.g., $U_{coh}/\sqrt{\Delta^2 S_\alpha'}$. The data-points represent, for each case, the quantum advantage estimated by the experimental frame-to-frame fluctuation in the absorption α determination, according to Eqs. (4) and (5), respectively. 300 shots and region where $\alpha \sim 1\%$ are used. The experimental classical uncertainty to compare with is obtained by the fluctuation of the estimate in Eq. (3), where the reference N_R is substituted by the mean value of the probe in the
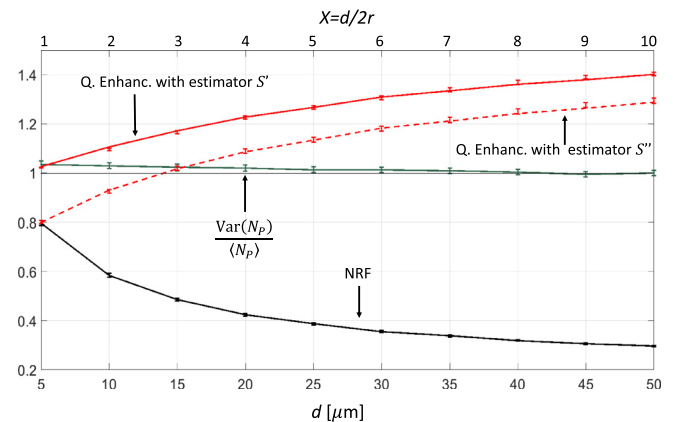
FIG. 2. Experimental *NRF* and quantum enhancement (as defined in the text) as a function of the spatial resolution in the object plane, d. The *NRF* (black data-series) is evaluated as $NRF = \Delta^2(N_P - N_R)/\langle N_P + N_R \rangle$ for photons numbers detected in an area of size d^2. Red data-series show the quantum enhancement provided by twin-beam (multimode TMSV states), both using the *Subtraction* estimation strategy, in Eq. (4) (dots, dashed line), or the *Optimized* one, in Eq. (5) (squares, solid line). The green data represent the quantity $\Delta^2 N_P/\langle N_P \rangle$ and confirm that the statistics of photon counts is Poissonian.
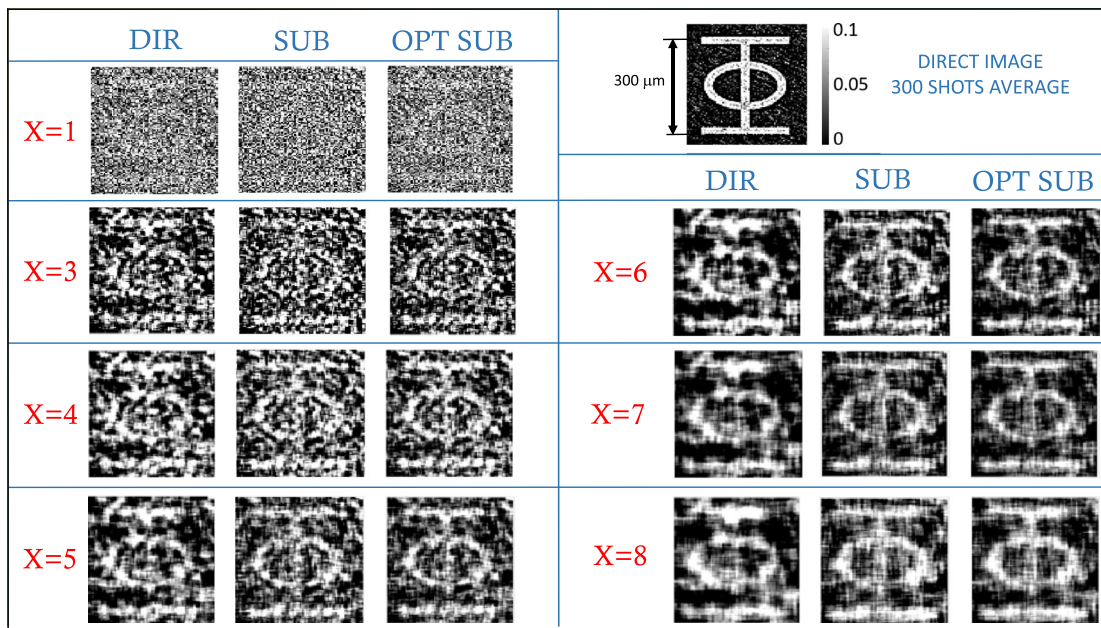
FIG. 3. Comparison between single shot images for different ratios X between the pixel dimension and the correlation diameter. For each X, the direct (DIR) image is compared with the image obtained using the quantum *Subtraction* protocol(SUB) and the one obtained using the *Optimized* protocol (OPT SUB). In the upper-right panel, the direct image of the object averaged over 300 shots is reported.

absence of the sample, $\langle N_P \rangle$. This estimator, using only the probe beam, reaches the lower classical bound U_{coh} of Eq. (1), substituting n_P with N_P, e.g., considering the same probe mean energy and detection efficiency as in the quantum strategy.[8]

As we have anticipated, the quantum advantage when using the subtraction estimator, as done in previous demonstration,[2] is present for $\eta > 0.5$ (red dashed line in Fig. 2). It corresponds to a resolution of 3 times the correlation length, namely, $15\,\mu m$. We can conclude that, with this estimator, it is not possible, even in principle, to have quantum enhancement and a resolution close to a single coherence length, at the same time.

In this context, using the *Optimized* estimator is a big opportunity because the quantum advantage of the twin-beam state can also be found for smaller values of the efficiency η or equivalently whenever $NRF \le 1$. In fact, the solid line in Fig. 2 shows that the quantum advantage is present also for $d = 5\,\mu m$, which is exactly the coherence length. Moreover, this estimator performs better than the other one for any resolution, always representing the best choice for SSNQI in wide-field modality.

As mentioned, the only point that deserves attention when using the *Optimized* estimator is that it requires a careful characterization of the experimental setup, in order to provide a reliable value of the parameter k_{opt} to insert in Eq. (5). This k_{opt} is a simple function of the excess noise and the detection efficiencies in both channels. We estimated the absolute quantum efficiency using a method that can be applied with an identical setup configuration.[24] We found that the performance of the *Optimized* estimator is not dramatically affected by the accuracy in the parameter's determination: few percent of uncertainty is enough to recover the advantage predicted by the theory.

Finally, in Fig. 3, we present a single frame experimental image of a specific absorbing mask for different spatial resolutions. The mask is realized by a thin "Φ-shaped" metallic deposition on a coated glass-slide with $\alpha \sim 1\%$. The resolution is set by the application of a median filter, which substitutes in each pixel (corresponding to $5\,\mu m$ in the object plane) the mean photon counts over a square of side d, centered in the pixel. As expected, the images obtained using the quantum protocol, i.e., using the twin-beam state, are visually better than the ones obtained by the single beam classical approach. Moreover, one can appreciate an improvement of the *Optimized* estimation protocol with respect to the *Subtraction* protocol in the residual noise level.

In this Letter, we have shown a substantial improvement of the performance of the SSNQI technique with respect to previous realization.[1,2,25] By studying different pure loss estimation strategies with quantum states of light in the presence of imperfections, we demonstrate that the robustness of an *Optimized* estimator with respect to detection losses and the link between spatial resolution and inefficiencies in detecting correlated photons imply that such an estimator produces a significant advantage also in terms of resolution. We have demonstrated that, different from the *Subtraction* protocol used in previous realizations, the limit to the resolution is given by the coherence area of the correlation in the far field of the SPDC process, which can be in principle reduced down to the Rayleigh limit determined by the numerical aperture of the optical system. This result represents a further step toward practical applications of quantum correlations in imaging and of using optimization techniques in this field.[26–33]

REFERENCES

[1] G. Brida, M. Genovese, and I. R. Berchera, "Experimental realization of sub-shot-noise quantum imaging," Nat. Photonics **4**(4), 227–230 (2010).

[2] N. Samantaray, I. Ruo-Berchera, A. Meda, and M. Genovese, "Realisation of the first sub shot noise wide field microscope," Light: Sci. Appl. **6**, e17005 (2017).

[3] O. Jedrkiewicz, Y. K. Jiang, E. Brambilla, A. Gatti, M. Bache, L. A. Lugiato, and P. Di Trapani, "Detection of sub-shot-noise spatial correlation in high-gain parametric down conversion," Phys. Rev. Lett. **93**, 243601 (2004).

[4] G. Brida, L. Caspani, A. Gatti, M. Genovese, A. Meda, and I. Ruo-Berchera, "Measurement of sub shot-noise spatial correlations without background subtraction," Phys. Rev. Lett. **102**, 213602 (2009).

[5] J. L. Blanchet, F. Devaux, L. Furfaro, and E. Lantz, "Measurement of sub-shot-noise correlations of spatial fluctuations in the photon-counting regime," Phys. Rev. Lett. **101**, 233604 (2008).

[6] E. Brambilla, L. Caspani, O. Jedrkiewicz, L. A. Lugiato, and A. Gatti, "High-sensitivity imaging with multi-mode twin beams," Phys. Rev. A **77**(5), 053807 (2008).

[7] M. Genovese, "Real applications of quantum imaging," J. Opt. **18**, 073002 (2016).

[8] E. Losero, I. Ruo-Berchera, A. Meda, A. Avella, and M. Genovese, "Unbiased estimation of an optical loss at the ultimate quantum limit with twin-beams," Sci. Rep. **8**, 7431 (2018).

[9] P. A. Moreau, J. Sabines-Chesterking, R. Whittaker, S. K. Joshi, P. M. Birchall, A. McMillan, J. G. Rarity, and J. C. F. Matthews, "Demonstrating an absolute quantum advantage in direct absorption measurement," Sci. Rep. **7**, 6256 (2017).

[10] D. Braun, G. Adesso, F. Benatti, R. Floreanini, U. Marzolino, M. W. Mitchell, and S. Pirandola, "Quantum enhanced measurements without entanglement," Rev. Mod. Phys. **90**(3), 035006 (2018).

[11] A. Monras and M. G. Paris, "Optimal quantum estimation of loss in bosonic channels," Phys. Rev. Lett. **98**(16), 160401 (2007).

[12] G. Adesso, F. Dell–Anno, S. De Siena, F. Illuminati, and L. A. M. Souza, "Optimal estimation of losses at the ultimate quantum limit with non-Gaussian states," Phys. Rev. A **79**(4), 040305 (2009).

[13] R. Nair, "Quantum-limited loss sensing: Multiparameter estimation and Bures distance between loss channels," Phys. Rev. Lett. **121**, 230801 (2018).

[14] A. Monras and F. Illuminati, "Measurement of damping and temperature: Precision bounds in Gaussian dissipative channels," Phys. Rev. A **83**(1), 012315 (2011).

[15] E. Jakeman and J. G. Rarity, "The use of pair production processes to reduce quantum noise in transmission measurements," Opt. Commun. **59**(3), 219–223 (1986).

[16] P. Tapster, S. Seward, and J. Rarity, "Sub-shot-noise measurement of modulated absorption using parametric down-conversion," Phys. Rev. A **44**, 3266 (1991).

[17] R. Whittaker, C. Erven, A. Neville, M. Berry, J. L. O'Brien, H. Cable, and J. C. F. Matthews, "Absorption spectroscopy at the ultimate quantum limit from single-photon states," New J. Phys. **19**(2), 023013 (2017).

[18] J. Sabines-Chesterking, "Sub-shot-noise transmission measurement enabled by active feed-forward of Heralded single photons," Phys. Rev. Appl. **8**, 014016 (2017).

[19] G. Brida, M. Genovese, A. Meda, and I. Ruo-Berchera, "Experimental quantum imaging exploiting multimode spatial correlation of twin beams," Phys. Rev. A **83**, 033811 (2011).

[20] I. N. Agafonov, M. V. Chekhova, T. Sh Iskhakov, A. N. Penin, G. O. Rytikov, and O. A. Shcherbina, "Absolute calibration of photodetectors: Photocurrent multiplication versus photocurrent subtraction," Opt. Lett. **36**(8), 1329–1331 (2011).

[21] M. Bondani, A. Allevi, G. Zambra, M. Paris, and A. Andreoni, "Sub-shot-noise photon-number correlation in a mesoscopic twin beam of light," Phys. Rev. A **76**, 013833 (2007).

[22] T. S. Iskhakov, V. C. Usenko, U. L. Andersen, R. Filip, M. V. Chekhova, and G. Leuchs, "Heralded source of bright multi-mode mesoscopic sub-Poissonian light," Opt. Lett. **41**, 2149–2152 (2016).

[23] A. Meda, E. Losero, N. Samantaray, F. Scafirimuto, S. Pradyumna, A. Avella, I. Ruo-Berchera, and M. Genovese, "Photon-number correlation for quantum enhanced imaging and sensing," J. Opt. **19**, 094002 (2017).

[24] A. Meda, I. Ruo-Berchera, I. P. Degiovanni, G. Brida, M. L. Rastello, and M. Genovese, "Absolute calibration of a charge-coupled device camera with twin beams," Appl. Phys. Lett. **105**, 101113 (2014).

[25] J. Sabines, A. McMillan, P. Moreau, S. Joshi, S. Knauer, E. Johnston, J. Rarity, and J. Matthews, "Twin-beam sub-shot-noise raster-scanning microscope with a hybrid detection scheme," arXiv:1906.05331.

[26] R. Gaiba and M. G. Paris, "Squeezed vacuum as a universal quantum probe," Phys. Lett. A **373**(10), 934–939 (2009).

[27] G. Brida, I. P. Degiovanni, A. Florio, M. Genovese, P. Giorda, A. Meda, M. G. A. Paris, and A. P. Shurupov, "Optimal estimation of entanglement in optical qubit systems," Phys. Rev. A **83**(5), 052301 (2011).

[28] C. Lupo and S. Pirandola, "Ultimate precision bound of quantum and subwavelength imaging," Phys. Rev. Lett. **117**(19), 190802 (2016).

[29] R. Nichols, P. Liuzzo-Scorpo, P. A. Knott, and G. Adesso, "Multiparameter Gaussian quantum metrology," Phys. Rev. A **98**(1), 012114 (2018).

[30] C. Lupo, Z. Huang, and P. Kok, "Quantum limits to incoherent imaging are achieved by linear interferometry," Phys. Rev. Lett. **124**(8), 080503 (2020).

[31] E. Losero, I. Ruo-Berchera, A. Meda, A. Avella, O. Sambataro, and M. Genovese, "Quantum differential ghost microscopy," Phys. Rev. A **100**(6), 063818 (2019).

[32] G. Ortolano, I. Ruo-Berchera, and E. Predazzi, "Quantum enhanced imaging of nonuniform refractive profiles," Int. J. Quantum Inf. **17**(8), 1941010 (2019).

[33] E. Knyazev, F. Y. Khalili, and M. V. Chekhova, "Overcoming inefficient detection in sub-shot-noise absorption measurement and imaging," Opt. Express **27**(6), 7868–7885 (2019).